Journal of Alloys and Compounds 480 (2009) L45–L48

Contents lists available at ScienceDirect

Journal of Alloys and Compounds

journal homepage: www.elsevier.com/locate/jallcom

Letter

Synthesis of $Er_2Ti_2O_7$ nanocrystals and its electrochemical hydrogen storage behavior

Lili Zhang[a,b], Weiguang Zhang[a,b], Junwu Zhu[a], Qingli Hao[a], Chao Xu[a], Xujie Yang[a], Lude Lu[a], Xin Wang[a,*]

[a] Key Laboratory for Soft Chemistry and Functional Materials, Nanjing University of Science and Technology, Ministry of Education, Nanjing 210094, China
[b] Department of Chemistry, Huaiyin Teachers College, Huai'an 223300, China

ARTICLE INFO

Article history:
Received 23 October 2008
Received in revised form 20 February 2009
Accepted 24 February 2009
Available online 13 March 2009

Keywords:
Energy storage materials
Sol–gel synthesis
Electrochemical reactions

ABSTRACT

Ultrafine $Er_2Ti_2O_7$ was synthesized at 700 °C within 2 h by a soft-chemistry route named citric acid sol–gel method (CAM). The obtained $Er_2Ti_2O_7$ with high dispersibility was square-like and the average size was about 70 nm. The prepared $Er_2Ti_2O_7$ nanocrystals in 6 M KOH aqueous solutions were investigated as a hydrogen storage material. It was found that the $Er_2Ti_2O_7$ powders would function as electrochemical hydrogen storage, showed fair electrochemical reversibility, and considerably high charge–discharge capacity. The reversible discharge capacity of the $Er_2Ti_2O_7$ electrode was found to exceed 320 mAh/g and adsorption capability of hydrogen is up to 1.27% at a current rate of 100 mA/g. In addition, the cycling ability and high rate capability of the $Er_2Ti_2O_7$ electrode are fairly good with only 4% capacity decay after 25 cycles. Cyclic voltammograms (CVs) were carried out to further examine the electrochemical hydrogen storage mechanism of $Er_2Ti_2O_7$.

1. Introduction

Recently, increasing efforts have been made in the search for new materials that allow hydrogen storage, including metal hydrides [1,2], metal alloys [1,3,4], carbon materials [1,5–8], semiconducting ceramics [1], perovskite-type oxides [8], etc. However, we found no report concentrating on the hydrogen storage property of pyrochlore-type oxides.

The pyrochlores have the general formula of $A_2B_2O_7$ where A is the larger cation and B is the smaller one. To the best of our knowledge, most of the pyrochlore oxides applications involved light, magnetism, and electricity fields [9–11], few reports were about pyrochlore oxides used as a catalyst [12] especially in photocatalytic system [13], but no papers related to its hydrogen storage property. In particular, many of these pyrochlore oxides undergo a high-temperature (1100–1400 °C) formation process and long-reaction time (1–2 d) [11,14], which is very energy and time consuming. So, attempts to synthesize nanoscale pyrochlore oxides under mild condition have been carried out by several soft-chemistry techniques, such as co-precipitation [15,16] and sol–gel methods [17,18]. In recent years, there have been some reports about how to fabricate pyrochlore oxides below 900 °C [19,20]. The fabrication route consumed an organic reagent, such as ethylene glycol, ethanol, etc. The fabricating temperatures were not so low; it was at least 800 °C. The aim of this article is to explore another simple and economical method to synthesize $Er_2Ti_2O_7$ nanocrystals at quite mild condition and study its electrochemical hydrogen storage property.

2. Experimental

2.1. Sample preparation and characterization

The synthesis route used in this research is named citric acid sol–gel method (CAM). Tetrabutyl titanate ($Ti(OBu)_4$) and Er_2O_3 were used as the precursors of Ti and Er. The molar ratio of Er/Ti was fixed at 1/1 and the amount of citric acid (CA) used was determined by $n_{CA}/(n_{Er}+n_{Ti})=2$.

Er_2O_3 (0.005 mol) was dispersed in a spot of water and then 5 mL concentrated HNO_3 was added to it drop by drop to dissolve the rare-earth oxide. Citric acid (0.04 mol) was dissolved in 5 mL H_2O, and then poured into the solution. The mixture was thoroughly stirred by the magnetic mixer.

Then the appropriate amount of $Ti(OBu)_4$ (0.01 mol) was added with vigorous stirring. After 0.5 h, a homogeneous transparent solution was formed. The solution was placed in an 80 °C liquid bath to vaporize water. Ten hours later, the mixture solution changed from colorless solution to yellow solution and then to transparent gel. The gel was then take out and calcined at 700 °C for 2 h in air.

The DTA–TG curves were evaluated on the Shimadzu DTA-50 thermal analysis instrument in ambient air and the calefactive velocity was 20 °C/min. The crystalline phase structure was determined by ARL/X/TRA X-ray diffractometer using Cu Kα radiation. The Brunauer–Emmett–Teller (BET) surface area was evaluated by N_2 adsorption in a constant volume adsorption apparatus (Coulter SA 3100). The morphology of product was determined by transmission electron microscopy (TEM) using JEOL-2100 microscopy and scanning electron microscopy (SEM) using LEO-1530VP SEM microscopy.

* Corresponding author. Tel.: +86 25 84315054; fax: +86 25 84315054.
E-mail address: wxin@public1.ptt.js.cn (X. Wang).

0925-8388/$ – see front matter © 2009 Elsevier B.V. All rights reserved.
doi:10.1016/j.jallcom.2009.02.146

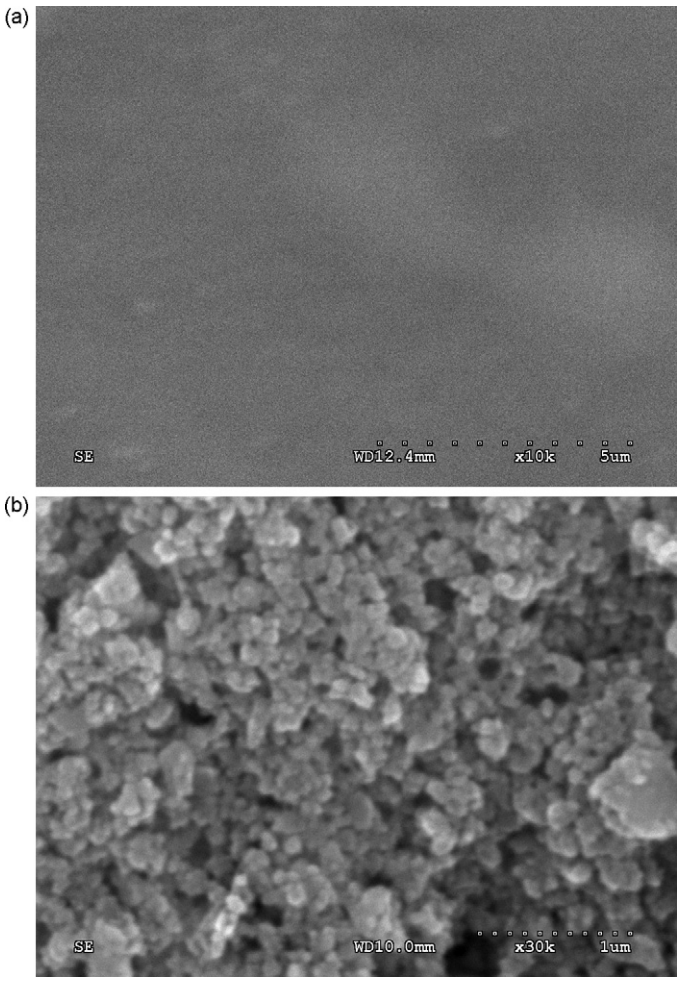

Fig. 1. SEM micrographs of the surface of bare GC electrode (a) and $Er_2Ti_2O_7$ modified on GC electrode (b).

2.2. Electrochemical hydrogen storage

Hydrogen charge/discharge performance of each sample was estimated with a three-electrode electrochemical cell at room temperature. In order to make a testing electrode, 33% $Er_2Ti_2O_7$ powder was mixed with 67% cuprum powder, pressed to a little flake at a pressure of 20 Mpa for 10 min, and then the obtained flake was sealed in a round copper disk. The charge/discharge capacity of $Er_2Ti_2O_7$ was tested in a three-electrode compartment (CT2001A LAND) using $Er_2Ti_2O_7$ electrode as cathode, a sintered nickel electrode as the counter electrode, and a Hg/HgO electrode as reference electrode in 6 mol/L KOH electrolyte at room temperature and normal atmosphere. The working electrodes were fully charged at constant current densities of 100 mA/g for 8 h and discharged at the current density of 50 mA/g after a rest of 10 min in both charge/discharge curves. The discharge cut-off potential relative to the Hg/HgO reference electrode was set to be −0.2 V.

The cyclic voltammetric (CV) experiments were performed on Autolab electrochemical analyzer (Eco Chemie, Holland) with a conventional three-electrode cell. The $Er_2Ti_2O_7$-modified glassy carbon (GC) electrode was used as working electrode; a Hg/HgO electrode as the reference and a platinum wire were used and the auxiliary electrode. A glassy carbon electrode (GCE, 3 mm in diameter) was polished to a mirror-like finish with fine emery papers and 1.0, 0.3, and 0.05 μm alumina slurry (Beuhler) followed by thoroughly rinsing with doubly distilled water. The electrode was then successively sonicated in alcohol and doubly distilled water, and allowed to dry at room temperature. To get the best CV responses of $Er_2Ti_2O_7$ films, the concentration of $Er_2Ti_2O_7$ was optimized at 2 mg/mL. Typically, 10 μL of the solution containing 0.02 mg $Er_2Ti_2O_7$ was spread evenly onto GC electrodes to prepare $Er_2Ti_2O_7$ films. The small bottle was fit tightly over the electrode so that water evaporated slowly and uniform films were formed. The modified electrode was rinsed twice with doubly distilled water to remove the non-firmly adsorbed $Er_2Ti_2O_7$. The obtained electrode was named as $Er_2Ti_2O_7$/GC-modified electrode. Then the CV experiment was carried out in 6 mol/L KOH solution and room temperature.

The SEM images of the GC electrode before and after the incorporation of $Er_2Ti_2O_7$ are given in Fig. 1. It can be seen that $Er_2Ti_2O_7$ was uniformly coated on the GC electrode surface. The $Er_2Ti_2O_7$ film has some "holes" or "channels" which allow the probe to go through the films and reach the electrode surface.

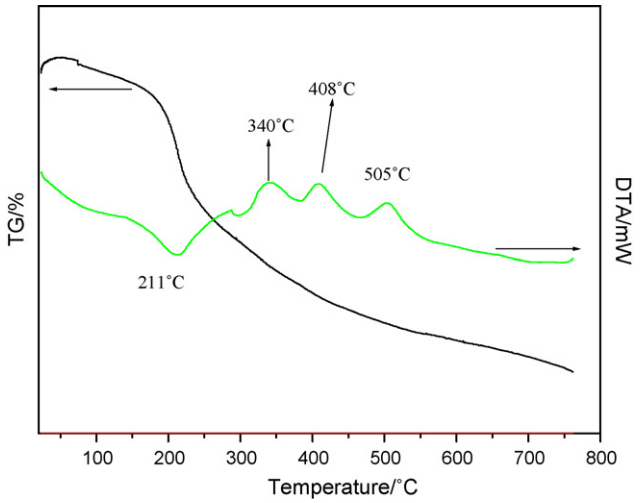

Fig. 2. DTA–TG curve of $Er_2Ti_2O_7$ precursor gel.

3. Results and discussion

3.1. Characterization of the $Er_2Ti_2O_7$

In order to confirm the fabricating temperature of $Er_2Ti_2O_7$ crystal, DTA–TG experiment was employed. Fig. 2 shows the DTA–TG curves of the precursor gel of $Er_2Ti_2O_7$. It can be seen that the DTA curve has four peaks. The first endothermic peak (211 °C) with relatively large weight loss (69.31%) is caused by the evaporation and burning of the organic substance. The second exothermic peak (340 °C) is attributed to the combustion of remaining organic substance and the third exothermic peak (408 °C) is related to the crystal lattice energy released during the formation of pyrochlore-type structure. The last exothermic peak is from the final formation of $Er_2Ti_2O_7$. The measured overall weight loss is 81.68%, which is quite consistent with the theoretical weight loss, and indicates the complete removal of all the citric acid and all the organic substance. No further weight loss was found up to 800 °C, suggesting the $Er_2Ti_2O_7$ can be fabricated at about 500 °C. The XRD patterns were identical to these.

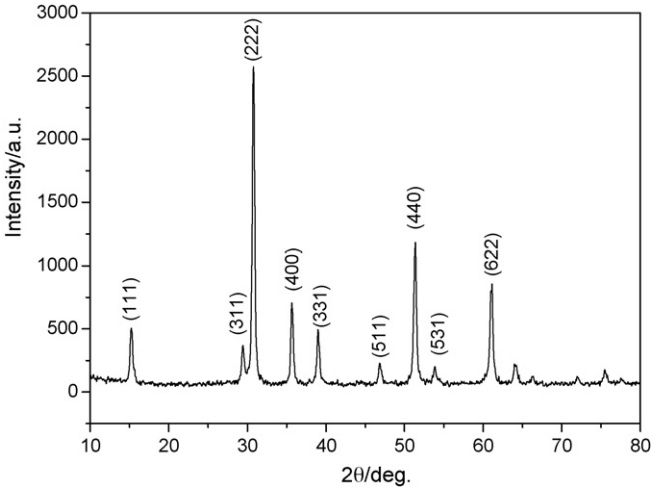

Fig. 3. XRD patterns of $Er_2Ti_2O_7$ calcined at 700 °C, 2 h by CAM.

Fig. 3 shows the XRD patterns of $Er_2Ti_2O_7$ powders prepared by CAM calcined at 700 °C (2 h). It is very clear that the crystallinity of the product is quite high, and XRD patterns were quite consistent to a single phase of pyrochlore $Er_2Ti_2O_7$, the XRD pattern is indexed based on face-centered cubic lattice (a = 10.23 Å) as observed previously (JCPDS 18-0499). These results suggest that the $Er_2Ti_2O_7$ pyrochlore oxide, usually forms at high temperature in conventional method (1100 °C) with a long reaction time (50 h) [5], can be successfully synthesized at a relatively low temperature (700 °C) with shortened reaction time (2 h) by using CAM. This technique has the benefit to reduce energy consumption and less environment pollution. It is a cheap and green route to achieve excellent pyrochlore oxide. Based on the Scherrer equation, the average size of $Er_2Ti_2O_7$ crystal was around 70 nm and this is quite consistent to the TEM results.

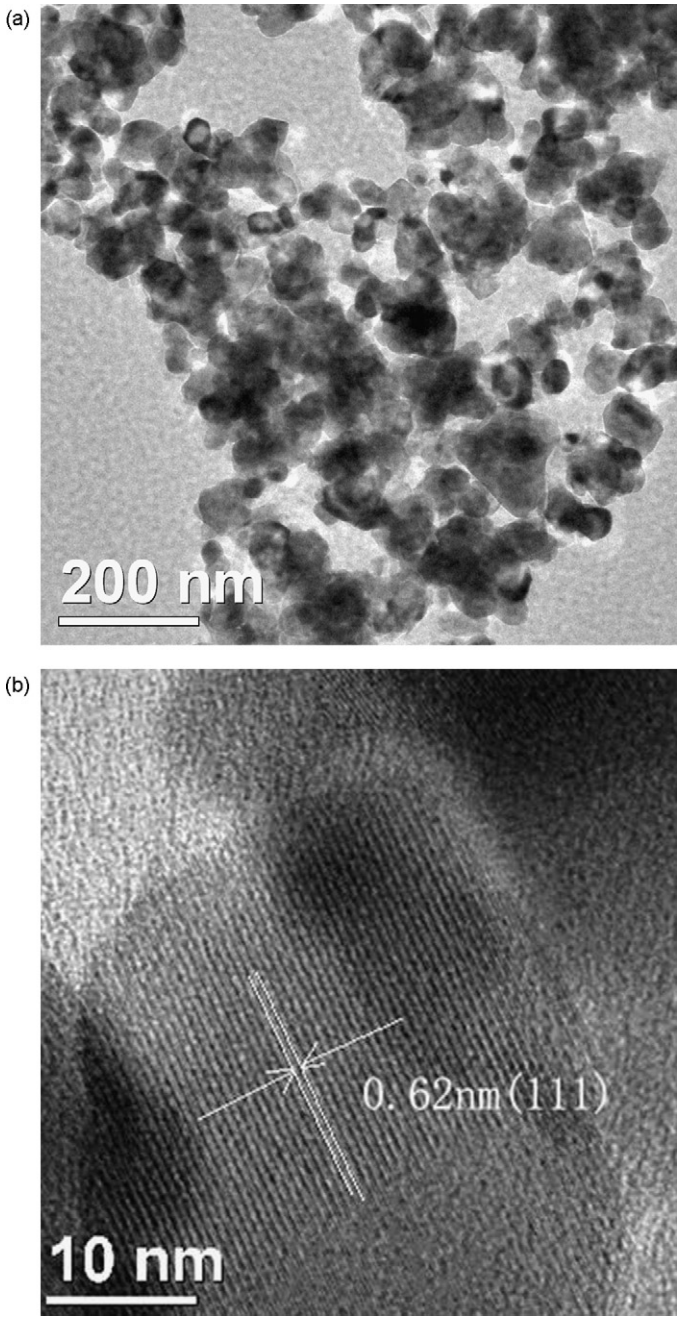

Fig. 4. TEM images of $Er_2Ti_2O_7$ (a) TEM and (b) HRTEM.

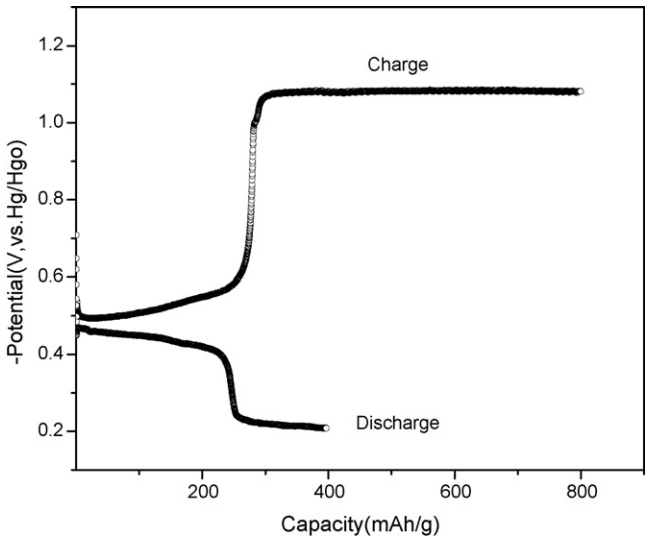

Fig. 5. Typical charge–discharge curves of $Er_2Ti_2O_7$ electrode.

Fig. 4 shows the TEM results of $Er_2Ti_2O_7$ prepared by CAM. From Fig. 4a, we can see the product of $Er_2Ti_2O_7$ crystalline is quadrilateral and with good dispersibility and the average size is about 70 nm, which is quite consistent to XRD results. In Fig. 4b, high-resolution transmission electron microscopy (HRTEM) image shows the clear and regular crystal lattice distance indicating that highly crystalline $Er_2Ti_2O_7$ was formed. The crystal lattice distance measured from the HREM images was 0.62 nm, which corresponds to (1 1 1)-lattice surface.

The BET surface area of $Er_2Ti_2O_7$ calculated from N_2 isotherms at 196 °C was 48.62 m^2/g, and is quite a bit larger than those of traditional solid-state reaction products (2–5 m^2/g) [10,19] and other soft-chemistry routes [11,17]. These good physical properties of the obtained sample by CAM, such as more regular morphology, higher dispersibility, and larger BET surface area may result in better behavior in hydrogen storage.

3.2. Electrochemical hydrogen storage of $Er_2Ti_2O_7$

To ensure the practical feasibility and cycling performance of $Er_2Ti_2O_7$ as a hydrogen storage electrode material, we constructed an experimental cell and carefully studied its electrochemical hydrogen storage behavior. Fig. 5 presents the typical charge–discharge curves of $Er_2Ti_2O_7$ electrode. As it is shown, the charge–discharge curves of the cell are similar to that of conventional hydrogen storage alloys [3], and the electrochemical discharge capacity is about 400 mAh/g.

Fig. 6 shows the cycling performance of $Er_2Ti_2O_7$ nanocrystals at a constant current density of 100 mAh/g at room temperature. The initial electrochemical discharge capacity of 345 mAh/g, corresponding to ~1.27 wt% hydrogen, was obtained in the $Er_2Ti_2O_7$ electrodes. During the 2nd to 10th cycle, the discharge capacities fluctuated and ranged from 420 to 330 mAh/g. This phenomenon may be caused by the interspaces between copper and $Er_2Ti_2O_7$ powders that resulted from the pressing process. Since copper and $Er_2Ti_2O_7$ powders have quite different conductivity, it needed quite some time to achieve the electric equilibrium, so the first 10 cycles were not so stable. This process may also be called an electrochemical activation process of $Er_2Ti_2O_7$, taken to achieve the intrinsic hydrogen storage capabilities of $Er_2Ti_2O_7$ electrode. From the tenth cycle and on, the reversible capacity was stabilized at ca. 320 mAh/g and the reversible capacity was still kept up at 310 mAh/g even after

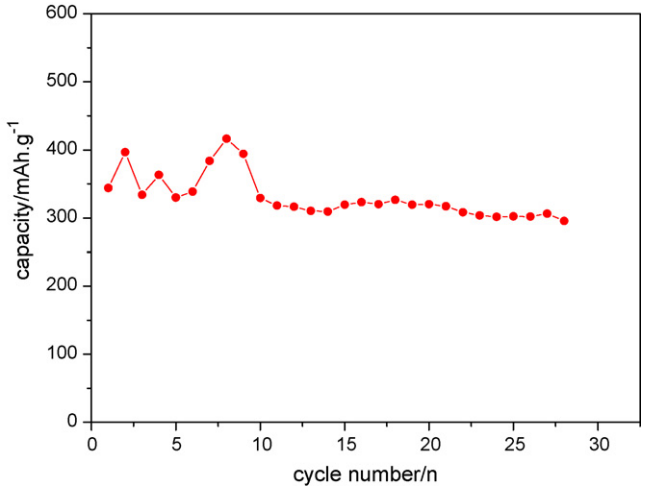

Fig. 6. Cycling performance of the $Er_2Ti_2O_7$ electrode at current densities of 100 mAh/g.

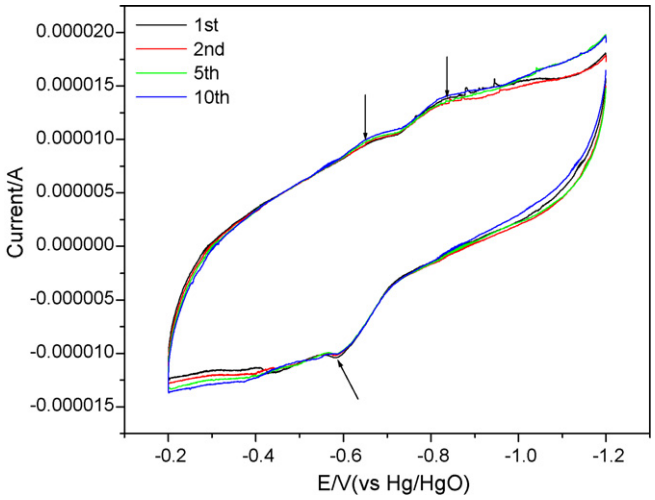

Fig. 7. Typical CV curves of the $Er_2Ti_2O_7$/GC electrode in a 6 M KOH solution. Potential sweep rate was set at 5 mV/s.

25 cycles, corresponding to 4% decaying, showing $Er_2Ti_2O_7$ powders possess quite good capacity retention.

Cyclic voltammograms (CVs) were carried out to further examine the electrochemical hydrogen adsorption–oxidation reactions of $Er_2Ti_2O_7$/GC electrode in 6 M KOH aqueous solutions. As shown in Fig. 7, the anodic oxidation peaks of hydrogen in the CVs are in a potential range between −0.5 and −0.6 V compared to Hg/HgO, and the cathodic adsorption peaks of hydrogen are observed to be around −0.8 V, which is quite similar to boron nitride nanotubes [21] and close to that of metal hydride electrodes and carbon nanotubes electrodes [22,23]. The desorption peaks of hydrogen appear near −0.7 V in the anodic process, indicating a slow desorption process of hydrogen at $Er_2Ti_2O_7$ electrode. The desorption peak of hydrogen appears prior to the electrochemical oxidation peak of hydrogen, suggesting the possible existence of the strong chemisorption of hydrogen [21].

At the same time, it was found that both the cathodic and anodic current were gradually increased along with the increasing of cycle number and tend to be consistent. This result is consistent to its charge/discharge property because of the electrochemical activation of $Er_2Ti_2O_7$. The increase in positive current is clear proof that water decomposition starts and produces hydrogen, which is immediately adsorbed on the surface of $Er_2Ti_2O_7$, and then electro-oxidized during the anodic sweep if the potential is higher than the equilibrium value.

Certainly, this description of the hydrogen storage mechanism of pyrochlore oxides is quite broad-brush, and further investigation will be concentrated on it.

4. Conclusions

$Er_2Ti_2O_7$ nanocrystals were synthesized at a relatively low temperature (700 °C) with shorten reaction time (2 h) by CAM. The hydrogen storage property of the prepared $Er_2Ti_2O_7$ was studied by electrochemical methods. Result show that $Er_2Ti_2O_7$ possess a promising reversible adsorption capability (up to 1.27%) and some charge/discharge capacity. The cycling ability of the $Er_2Ti_2O_7$ electrode is fairly good with only 4% capacity decay after 25 cycles. Cyclic voltammograms (CVs) were carried out to further examine the electrochemical hydrogen storage mechanism of $Er_2Ti_2O_7$. This research could be very helpful to develop new material in hydrogen storage system.

Acknowledgments

The authors thank the National Natural Science Foundation of China (50572039), Postdoctoral Science Foundations of China (20060400941) and Jiangsu Province (0602003A), College Natural Science Foundation (07KJB430010), Impellent Industrialization program of College Research Achievement (JH08-31) of Jiangsu Province, Doctoral Foundation of Huaiyin Teachers College (07HSBS005), and Technological Research Foundation of Huai'an City (HAG08072) for financial support.

References

[1] A.M. Seayad, D.M. Antonelli, Adv. Mater. 16 (2004) 765–777.
[2] A.R. Akbarzadeh, V. Ozoliņš, C. Wolverton, Adv. Mater. 19 (2007) 3233.
[3] Y.D. Wang, X.P. Ai, H.X. Yang, Chem. Mater. 16 (2004) 5194–5197.
[4] H.G. Pan, Y.F. Liu, M.X. Gao, et al., J. Alloys Compd. 351 (2003) 228–234.
[5] H.Y. Zhang, X.J. Fu, Y.M. Chen, et al., Physica B 352 (2004) 66–72.
[6] B.Z. Fang, H.S. Zhou, I. Honma, J. Phys. Chem. B 110 (2006) 4875–4880.
[7] K. Jurewicz, E. Frackowiak, F. Beguin, Appl. Phys. A 78 (2004) 981–985.
[8] T. Esaka, H. Sakaguchi, S. Kobayashi, Solid State Ionics 166 (2004) 351–357.
[9] A.V. Shlyakhtina, A.V. Knotko, M.V. Boguslavskii, et al., Solid State Ionics 176 (2005) 2297–2304.
[10] V.V. Nemoshkalenko, V.N. Uvarov, S.V. Borisenko, et al., J. Electron Spectrosc. Relat. Phenom. 88–91 (1998) 385–390.
[11] M. Uno, A. Kosuga, M. Okui, et al., J. Alloys Compd. 400 (2005) 270–275.
[12] J.M. Sohn, M.R. Kim, S.I. Woo, Catal. Today 83 (2003) 289–297.
[13] L.L. Zhang, H. Zhong, W.G. Zhang, et al., J. Alloys Compd. 463 (2008) 466–470.
[14] F.X. Zhang, B. Manoun, S.K. Saxena, Mater. Lett. 60 (2006) 2773–2776.
[15] J. Takahashi, T. Ogtsuka, J. Am. Ceram. Soc. 72 (1989) 426–429.
[16] J. Takahashi, K. Kageyarna, K. Kodaira, Jpn. J. Appl. Phys. 32 (9B) (1993) 4327–4330.
[17] A.V. Prasadarao, U. Selvaraj, S. Komarneni, et al., Mater. Lett. 12 (1991) 306–310.
[18] A.V. Prasadarao, U. Selvaraj, S. Komarneni, et al., J. Mater. Res. 7 (1992) 2859–2863.
[19] A. Garbout, S. Bouattour, M. Ellouze, et al., J. Alloys Compd. 425 (2006) 88–95.
[20] M.M. Milanova, M. Kakihana, M. Arima, et al., J. Alloys Compd. 242 (1996) 6–10.
[21] X. Chen, X.P. Gao, H. Zhang, et al., J. Phys. Chem. B 109 (2005) 11525–11529.
[22] X. Qin, X.P. Gao, H. Liu, H.T. Yuan, D.Y. Yan, W.L. Gong, D.Y. Song, Electrochem. Solid-State Lett. 3 (2000) 532–536.
[23] X.P. Gao, J. Liu, S.H. Ye, D.Y. Song, Y.S. Zhang, J. Alloys Compd. 253–254 (1997) 515–519.